Available online at www.sciencedirect.com
SCIENCE DIRECT®
Journal of Banking & Finance 28 (2004) 1499–1520
Journal of BANKING & FINANCE
www.elsevier.com/locate/econbase

A new approach to modeling the dynamics of implied distributions: Theory and evidence from the S&P 500 options

Nikolaos Panigirtzoglou [a], George Skiadopoulos [b,c,*]

[a] *Monetary Instruments and Markets Division, Bank of England, Threadneedle Street, London EC2R 8AH, UK*
[b] *Department of Banking and Financial Management, University of Piraeus, Karaoli & Dimitriou 80, Piraeus 18534, Greece*
[c] *Financial Options Research Centre, Warwick Business School, University of Warwick, UK*

Received 17 October 2002; accepted 31 March 2003
Available online 4 July 2003

Abstract

This paper presents a new approach to modeling the dynamics of implied distributions. First, we obtain a parsimonious description of the dynamics of the S&P 500 implied cumulative distribution functions by applying principal components analysis. Subsequently, we develop new arbitrage-free Monte Carlo simulation methods that model the evolution of the whole distribution through time as a diffusion process. Our approach generalizes the conventional approaches of modeling only the first two moments as diffusion processes, and it has important implications for "smile-consistent" option pricing and for risk management. The out-of-sample performance within a Value-at-Risk framework is examined.

JEL classification: G11; G12; G13
Keywords: Implied distribution; Monte Carlo simulation; Option pricing; Principal components analysis; Value-at-Risk

* Corresponding author. Address: Department of Banking and Financial Management, University of Piraeus, Karaoli & Dimitriou 80, Piraeus 18534, Greece.
E-mail addresses: nikolaos.panigirtzoglou@bankofengland.co.uk (N. Panigirtzoglou), gskiado@unipi.gr (G. Skiadopoulos).

0378-4266/$ - see front matter
doi:10.1016/S0378-4266(03)00127-4

1. Introduction

Cross-sections of option prices can be used to infer (imply) the risk-neutral probability density function (PDF or the equivalent cumulative distribution function, CDF) for the future values of the underlying asset. There is an extensive literature on methods to extract the implied PDF at a *single point* in time. The objective of this paper is to investigate the *dynamics* of implied distributions, and to provide algorithms that can apply the empirical results to areas like option pricing and risk management.

Over the last 25 years, there has been a considerable interest among academics, market participants, and policy makers to extract information from option prices regarding the market participants expectations (see Jackwerth (1999) and Mayhew (1995) among others for surveys on the techniques have been developed to estimate the risk-neutral PDF). The extracted PDFs are used as a guide to economic policy issues such as assessing monetary credibility, revealing the public's expectations about future interest rates, and evaluating the timing of monetary policy actions (see for example, Neuhaus, 1995; Söderlind and Svensson, 1997). They are also used to test whether specific events (e.g., the '87 crash, or the outcome of elections) were expected (see Bates, 1991; Gemmill and Saflekos, 2000; Coutant et al., 2001).

Even though the estimation of the implied distributions at a *single* point in time has been studied thoroughly, we are not aware of any attempt to empirically explore *and* model *explicitly the stochastic evolution of the whole PDF through time*. [1] So far, researchers in finance have been modeling the first two moments of the distribution, either in a static framework (e.g. a single factor standard capital asset pricing model, CAPM or in a dynamic one e.g. Black and Scholes type of model, stochastic volatility option pricing models). However, the empirical evidence shows that higher-order moments should be modeled, as well; Bates (1991, 1996) and Lynch and Panigirtzoglou (2003) find that the skewness and kurtosis of implied distributions change considerably over time. Recent studies (e.g., Fama and French, 1992) indicate that the CAPM cannot explain the cross-asset variation in expected returns, leaving space for introducing additional variables. Towards this direction, Harvey and Siddique (2000) develop an asset pricing model that incorporates the (conditional) skewness. Modeling the entire distribution is the most general approach one can take, so as to capture the effect of higher-order moments, as well.

[1] So far, the stochastic evolution of implied distributions has been modeled only indirectly (see Bates, 2003, for a discussion). This is done via the equivalent methods of modeling implied volatilities (Ledoit and Santa-Clara, 1998; Schönbucher, 1999), or local volatilities (e.g., Derman and Kani, 1998), or option prices (Britten-Jones and Neuberger, 2000). Empirical studies such as Kamal and Derman (1997), Skiadopoulos et al. (1999), Alexander (2001a,b), Ané and Labidi (2001), Fengler et al. (2001), and Cont and Da Fonseca (2002) have also investigated the dynamics of implied distributions implicitly, by examining the properties of implied volatilities. On the other hand, Skiadopoulos and Hodges (2001) simulate the evolution of the implied distribution explicitly, without relying on any empirical evidence. Lynch and Panigirtzoglou (2003) study only the time series properties of the implied PDFs summary statistics.

Furthermore, understanding and modeling the dynamics of implied distributions may allow us to address a number of issues in financial economics such as market microstructure questions, option pricing and risk management problems. In particular, the evolution of implied PDFs can be viewed as a result of changes in the market participants information set. Hence, the implications of various microstructure models can be examined, e.g., Kyle's (1985) model implication that more information is revealed in the market as the volume increases.

Developing a theory about the dynamics of implied distributions can be helpful for "smile-consistent" option pricing and hedging when the moments of the distribution change in a *stochastic* way. "Smile-consistent" models (also called "implied models") take the prices of traded plain vanilla options as given, and they use them to price exotic and illiquid options. [2] Implied distributions reflect the same information as the traded option prices. In addition, option prices can be obtained by integrating their payoffs over the risk-neutral distribution. Therefore, starting from today's distribution, the stochastic evolution of the implied distribution is equivalent to the consistent with the smile *stochastic evolution* of option prices.

Knowledge of the evolution of implied distributions is also useful for risk management purposes such as Value-at-Risk (VaR). VaR is the loss that corresponds to a given probability over a pre-specified time horizon. Ait-Sahalia and Lo (2000) define as Economic-VaR (E-VaR) the VaR calculated from the implied risk-neutral distribution. They have proposed it as a forward-looking measure of risk compared to the conventional VaR measures calculated from the actual distribution (see also Lo (1999), for a discussion of the merits of such a measure). Consequently, the dynamics of implied distributions reveal the variation of (risk-neutral) VaR over time.

In this paper, initially we investigate the dynamics of three *constant*-maturity S&P 500 implied CDFs by applying principal components analysis (PCA). We use a variety of criteria in order to determine the number of factors that explain the evolution of implied distributions through time. We obtain a parsimonious description of the dynamics of implied distributions since we identify two components that explain 89–92% of the variance depending on the maturity.

Subsequently, the implied distribution is modeled as a diffusion process. We develop two new Monte Carlo (MC) simulation algorithms that model the evolution of the implied PDF and of the implied CDF over time, respectively. The presented methods are *arbitrage-free*. Our modeling approach is new. It can be regarded as the generalization of the conventional approaches of modeling only the first two moments of the implied distribution as diffusion processes. It differs from the approach suggested by Skiadopoulos and Hodges (2001) who first performed MC simulation

[2] "Smile-consistent" models fall within two categories: deterministic, and stochastic volatility "smile-consistent" models. The former category assumes that volatility is a deterministic function of the asset price and time. The latter assumes that volatility evolves stochastically. Dumas et al. (1998) and Buraschi and Jackwerth (2001) have shown that "smile-consistent" deterministic volatility models cannot forecast accurately the stochastic evolution of option prices over time. Hence, "smile-consistent" stochastic volatility models is the next natural candidate to capture the stochastic evolution of option prices over time (see Jackwerth (1999) and Skiadopoulos (2001) for a review of "smile-consistent" models).

of implied distributions. Their algorithm simulates the implied distribution by assuming that sequential shocks affect the first two moments of the distribution. Then, a mixture of distributions is specified so as to capture the effect of a shock to any given moment.

The proposed algorithms require as inputs only the initial implied distribution and the volatility shocks of the process (i.e. the PCA results). Modeling the dynamics of implied distributions by using the PCA results is analogous to implementing Heath et al. (1992) type of models using PCA. In the context of smile-consistent option pricing with stochastic volatility, we show that the simulation of the implied distribution is preferable to the simulation of local, or implied volatilities. This is because it avoids the problems associated with the calculation of the drift of the process of local volatilities (as it is the case in Derman and Kani's, 1998, model), or those associated with the estimation of the implied volatility process (e.g., in Ledoit and Santa-Clara's, 1998, model). On the other hand, the algorithms cannot be used for the pricing of American options as it is the case with the conventional Monte Carlo simulation, and for the simultaneous pricing of options having different expiries.

Finally, we test the out-of-sample performance of the algorithm that simulates the implied CDF, within a E-VaR framework. Using the historically estimated PCA factors, the algorithm is applied to forecast the variability of an extreme initial implied probability that corresponds to a given horizon's E-VaR level (probability E-VaR). We find that the algorithm forecasts accurately the range within which the future probability E-VaR will lie. The results have important implications for the economics of option pricing.

The remainder of the paper is structured as follows. First, we present the data set used, and explain the method we chose to extract the implied distributions. The metric under which implied distributions are measured, is discussed. In Section 3 we describe the PCA technique including why it was chosen, and how it will be applied to analyze the data. Next, the dynamics of the implied CDFs are explored. In Sections 5 and 6, we develop the methods for the simulation of the implied PDF and CDFs, respectively. In Section 7, the test of the out-of-sample performance is explained, and results are presented. In the last section, we conclude with a brief summary, certain implications of this paper are discussed, and we suggest directions for future research.

2. The data set

2.1. Source data description

The raw dataset contains the daily settlement prices of the S&P 500 futures options and of the underlying futures contracts traded in the Chicago Mercantile Exchange (CME) for the period from 19/06/98 to 29/12/2001.

The CME S&P 500 options contract is an American style futures option; the underlying future is the CME S&P 500 futures contract. S&P 500 options trade with

expiries on the same expiry dates as the underlying futures contract. These trade out to one year with expiries in March, June, September and December. In addition, there are monthly serial option contracts out to one quarter. Options expire on the 3rd Friday of the expiry month, as do the futures contracts in their expiry months. Options quotations used to compute PDFs are the settlement prices, and the associated price of the underlying is the settlement price of the S&P 500 futures contract maturing on, or just after, the option expiry date.

2.2. Extracting the implied distributions

We estimate the implied PDFs using the non-parametric method presented in Bliss and Panigirtzoglou (2002). This method is chosen because it generates PDFs that are robust to quite significant measurement errors in the quoted option prices, as shown in Bliss and Panigirtzoglou (2002) (see also McIntyre (2001) for an implicit discussion of the effect of data limitations on the extracted implied probabilities). The technique makes use of Breeden and Litzenberger (1978) non-parametric result, and it uses a natural spline to fit implied volatilities as a function of the deltas of the options in the sample.

Breeden and Litzenberger (1978) showed that assuming that option prices are observed across a continuum of strikes, the second derivative of a European call price with respect to the strike price delivers the risk neutral PDF. However, in practice, available option quotes do not provide a continuous call price function. To construct such a function, a smoothing function (natural spline) is fitted in the implied volatility space. We calculate implied volatilities from option prices by using the analytical quadratic approximation of Barone-Adesi and Whaley (BAW, 1987). This is an accurate and computationally efficient modification of the Black–Scholes formula that captures the early exercise premium of the American-style S&P 500 futures options. In addition, the implied volatility calculated via the BAW formula can be inserted in the Black–Scholes formula to calculate the European option prices (see BAW, 1987, for a discussion). Hence, Breeden and Litzenberger's result that was derived for European options can also be applied to our American option data set.

For the purposes of calculating implieds, the standard filtering constraints were imposed. Only at-the-money and out-of-the-money options were used because they are more liquid than in-the-money. Hence, measurement errors in the calculation of implied volatilities due to non-synchroneity (Harvey and Whaley, 1991) and bid–ask spreads are less likely to occur because their delta is smaller than that of in-the-money options. Option prices that violate the monotonicity and convexity no-arbitrage property of the call/put pricing function were discarded. Option prices with less than five working days to maturity were also excluded; these prices are excessively volatile as market participants close their positions. Options for which it was impossible to compute an implied volatility were discarded. The three-month LIBOR interest rates taken from Bloomberg, are used for the calculation of implied volatilities. The choice of the interest rate does not introduce any noise in the calculation of implied volatilities because rho is very small for out-of-the-money options.

The delta metric is constructed by converting strikes into their corresponding call deltas by using the at-the-money implied volatility. [3] Hence, a set of implied volatilities and corresponding deltas is constructed for each available contract. Implied volatilities of deltas greater than 0.99 or less than 0.01, are discarded. These volatilities correspond to far out-of-the-money call and put prices, which have generally low liquidity. An implied volatility smile is constructed if there are at least three implied volatilities, with the lowest delta being less than or equal to 0.25 and the highest delta being greater than or equal to 0.75. This ensures that the available strikes cover a wide range of the PDF available outcomes. In the case that the range of strikes does not spread along the required interval, no PDF is extracted.

Once the spline is fitted, 20,000 points along the function are converted back to option price/strike space using BAW approximation. Finally, the 20,000 call price/strike data points are used to differentiate numerically the call price function so as to obtain the estimated PDF for the cross-section.

2.3. Constructing constant horizon implied distributions

The S&P 500 option contracts have fixed expiry dates, that is, the time to maturity changes with time. This poses a problem to the purposes of our analysis. As the option contract approaches its expiry, the implied distribution will degenerate. We want to exclude this "time-to-maturity" effect from studying the dynamics of implied PDFs. Hence, we construct *constant-horizon* PDFs by using the extracted implied PDFs. The construction of constant-horizon probabilities is done as described in Clews et al. (2000) (see also Coutant et al., 2001, for a similar approach).

We construct implied CDFs for constant maturities $T = 1$, 3 and 6 months. For the purposes of our analysis, implied CDFs are measured in a call delta metric; this is constructed as described above. Hence, the state probabilities correspond to the formed at time t cumulative probabilities $\pi_t(X(\delta), T) \equiv \text{Prob}[S_T \leqslant X(\delta)]$, where $X(\delta)$ corresponds to a strike of a particular delta δ with T time-to-maturity, and $t < T$. We have calculated cumulative probabilities $\pi_t(X(\delta), T)$ for strikes $X(\delta)$ of 21 different deltas δ (0.01, 0.059, ..., 0.5, ..., 0.941, 0.99) for every T.

The advantage of measuring implied distributions on a (call) delta metric is that the delta variables are constrained in the interval [0,1]. Therefore, we can capture the entire area of the distribution by using a small number of variables, as opposed to using an alternative metric (e.g. a futures Profit/Loss metric). The reduction in the number of variables will increase the effectiveness of our subsequent PCA. In addition, the delta metric adjusts the changes in probabilities of the states $S_T \leqslant X(\delta)$ to changes in the level of the underlying asset, to changes in the volatility, and to

[3] A small delta corresponds to a high strike (i.e. out-of-the-money calls), while a large delta corresponds to a low strike (i.e. in-the-money calls). The formula for transforming each strike into a delta is the Black's model delta. We use the at-the-money implied volatility so as the ordering of deltas is the same as that of the strikes. Using the implied volatilities that correspond to each strike could change the ordering in the delta space, in cases where steep volatility skews are observed. This would result in generating volatility smiles with artificially created kinks.

changes in the time to maturity. Due to its latter characteristic, Kamal and Derman (1997) have employed the delta metric to analyze the dynamics of implied volatilities. For the same reason, currency option traders also quote option prices in terms of implied volatilities measured as a function of delta (see Malz, 1997).

3. Principal components analysis and implied distributions

We outline the PCA methodology used in this paper. PCA is used to explain the systematic behavior of observed variables, by means of a smaller set of unobserved latent random variables. Its purpose is to transform p correlated variables to an orthogonal set which reproduces the original variance–covariance structure (or correlation matrix).

PCA has been used in the interest rate literature to explore the dynamics of the yield curve and to provide alternative hedging schemes to the traditional duration hedge (see Knez et al., 1994, among others). Kamal and Derman (1997), Skiadopoulos et al. (1999), Alexander (2001a), Ané and Labidi (2001), Fengler et al. (2001), and Cont and Da Fonseca (2002) have applied PCA to investigate the dynamics of implied volatilities (see also Alexander (2001b) for an extensive description of the applications of PCA in finance). We apply PCA to decompose the correlation structure of first differences of implied CDFs. To achieve this, we measure the daily differences of implied CDFs across different levels of delta for each one of the three different fixed maturities. [4] This will shed light on whether the dynamics of distributions depend on the maturity we examine.

Next, a separate PCA on the first differences of implied CDFs is performed for each maturity. This is because we tested for unit-roots by applying standard Dickey–Fuller tests to time series of the levels of CDFs for a given constant-maturity and delta. We found that the null hypothesis of the existence of unit-root cannot be rejected. In addition, we calculated the means (and their t-statistics) of the daily CDF differences across different deltas and maturities. We found that the average constant-maturity CDF differences are not significantly different from zero. Hence, implied CDFs need to be differenced so as to remove the non-stationarity; Frachot et al. (1992) have shown that PCA is misleading when applied to non-stationary variables. We perform PCA on a data set over the period 19/06/98 to 29/12/2000. [5] The data for year 2001 will be used for an out-of-sample test of the PCA (see Section 7).

[4] We applied PCA to the "percentage futures Profit/Loss" metric $P/L = (F_T - F_t)/F_t$, where F_t is the futures price observed at time t, and F_T is the futures price at the option's maturity. However, the PCA on P/L gave rather noisy results compared to the delta metric analysis. Therefore, we only report the results obtained from applying PCA to the delta metric.

[5] The first order autocorrelations of the daily CDF differences across the different deltas and maturities were also calculated. We found evidence of a fairly minor negative first-order autocorrelation; this was −0.22, −0.18, −0.19 on average across the deltas, for the one, three, and six months maturity, respectively. However, this does not pose a problem to the reliability of the subsequent PCA; Skiadopoulos et al. (1999) have found that the presence of autocorrelation does not hamper the efficiency of the PCA.

The general PCA setup can be described as follows. Denote time by $t = 1, \ldots, K$ and let p be the number of variables. Such a variable is a $(K \times 1)$ vector $\mathbf{l}$. In our framework, $p = 21$, and each variable $\mathbf{l}$ is a time series collection of differences in implied CDFs for a given delta level and within a constant maturity. The purpose of the PCA is to construct p principal components (PCs hereafter) as linear combinations of the vectors $\mathbf{l}$, orthogonal to each other, which reproduce the original variance–covariance structure. In matrix notation,

$$\mathbf{L} = \mathbf{Z}\mathbf{A}', \tag{1}$$

where $\mathbf{L}$ is a $(K \times p)$ matrix, $\mathbf{Z}$ is a $(K \times p)$ matrix of PCs, and $\mathbf{A}$ is a $(p \times p)$ matrix of loadings. When both variables and components are standardized to unit length, the elements of $\mathbf{A}'$ are correlations between the variables and PCs and they are called *correlation loadings* (see Basilevsky, 1994, for more details). If we retain $r < p$ PCs then

$$\mathbf{L} = \mathbf{Z}_{(r)}\mathbf{A}'_{(r)} + \boldsymbol{\varepsilon}_{(r)}, \tag{2}$$

where $\boldsymbol{\varepsilon}_{(r)}$ is a $(K \times p)$ matrix of residuals and the other matrices are defined as before having r rather than p columns. The percentage of variance of $\mathbf{l}$ which is explained by the retained PCs (*communality* of $\mathbf{l}$) is calculated from the correlation loadings. After retaining $r < p$ components, we look at Eq. (2) to examine the size of the communalities, and the meaning of the retained components.

4. Principal component analysis on implied cumulative distribution functions

In this section, we investigate the dynamics of implied distributions by applying PCA to implied cumulative distribution functions. Working with CDFs rather than with probability density functions has the advantage that we can capture the entire PDF through a mapping from [0,1], the range of call delta values, to [0,1], the range of CDF values. We decide on the number of components to be retained and we look at their interpretation.

4.1. Number of retained principal components and their interpretation

We determine the number of components to be retained by looking at a range of criteria. [6] First, we apply Velicer's (1976) non-parametric criterion. [7] Next, working

[6] Knez et al. (1994) apply PCA to the yield curve and they retain three components because these are explaining about 98% of the total variance. However, as Jackson (1991, p. 44) notes "this procedure is not recommended. There is nothing sacred about any fixed proportion" (see also Basilevsky, 1994, for similar comments). For a description and discussion of the several rules of thumb, see Jackson (1991).

[7] Most of the tests used for determining the number of PCs to be retained, are parametric based on the assumption of multivariate normality (for a review of these tests, see Basilevsky, 1994). However, application of Q–Q plots to our dataset, showed that the null-hypothesis of univariate, and hence of multivariate normality, was rejected. Therefore, we decided to use a non-parametric method.

Table 1
Principal components from the PCA on implied cumulative distributions: r^* = the number of components retained under Velicer's criterion (minimum of $f_0, \ldots, f_4$)

	f_0	f_1	f_2	f_3	f_4	r^*	1st PC	2nd PC	3rd PC
1 month	0.46218	0.46192	0.46203	0.46214	0.46217	1	65.17%	23.70%	7.95%
3 months	0.45711	0.45696	0.45702	0.45708	0.45710	1	62.51%	30.12%	4.74%
6 months	0.44224	0.44211	0.44214	0.44221	0.44222	1	60.95%	30.87%	5.44%

with components retained under this criterion, we look at the communalities. Finally, we look at the interpretation of the PCs. If any component appears to be noise then we prefer to reject it.

Velicer proposes a non-parametric method for selecting nontrivial PCs, i.e. components which have not arisen as a result of random sampling, measurement error, or individual variation. His method is based on the partial correlations of the residuals of the PCs model, after $r < p$ components have been extracted (see also Skiadopoulos et al., 1999, for a description of the test).

Table 1 shows the retained PCs under Velicer's criterion when the PCA has been performed on implied CDFs. We can see that according to this criterion one component is retained for each maturity. The first two PCs explain on average 91% of the total variation of implied CDFs, across the three constant maturities.

We check the goodness-of-fit to probabilities (i.e., to option prices) of the first two PCs by examining their communalities; the communalities of the first PC are compared to the communalities that the first two components explain. We find that the first PC alone give rise to low communalities (almost zero) for some deltas. Including the second PC increases the explained communalities to more than 90% in most of the deltas. The communality criterion indicates that two components should be retained.

As a final step in our methodology for the number of components to retain, we look at the interpretation of the first three components. Fig. 1 shows the correlation loadings of the first three PCs across the three maturities as these have been obtained from the PCA on implied CDFs. For middle deltas, the first PC has almost equal size correlation loadings. For very low and high deltas the size of the correlation loadings decreases. This attenuation is stronger for the nearest contract. Assuming a positive sign for the first shock, these results imply that it accumulates more probability mass in the center of the CDF and less mass at the edges. The second PC accumulates more mass in the lower part of the CDF; in the middle part the mass reduces, and then it increases again. The third PC has a rather noisy behavior. This confirms that two components drive the dynamics of the implied CDFs. Table 2 shows descriptive statistics (minimum, maximum, skewness, and kurtosis) of the time series behavior of the first two principal components across the three constant maturities. We can see that the distribution of the two PCs has zero skewness and high kurtosis. This implies that large shocks of either sign are equally likely to happen. We comment further on the importance of this finding in Section 7.3.

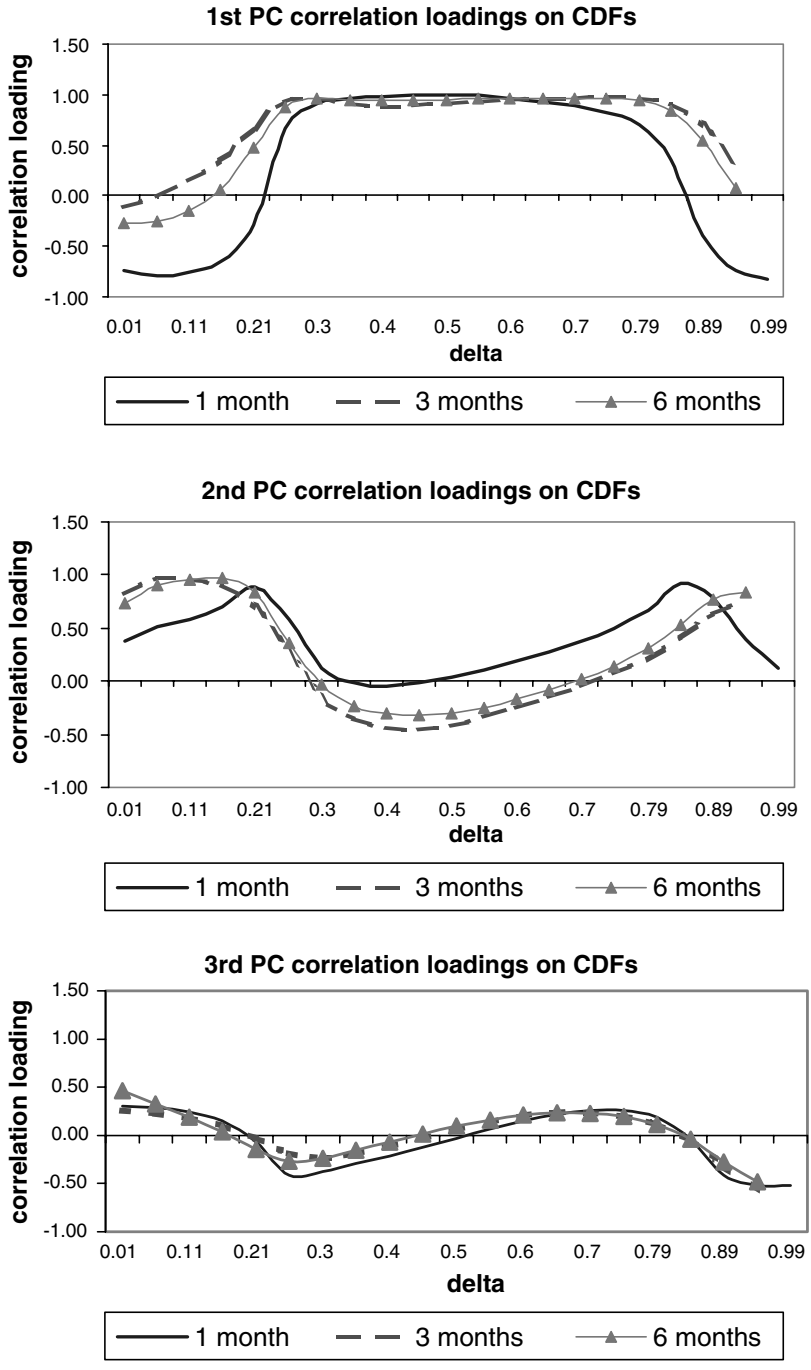

Fig. 1. PCA on implied CDFs: Correlation loadings of the 1st, 2nd, and 3rd PC across the one, three, and six-months constant maturities.

Table 2
Descriptive statistics (minimum, maximum, skewness, kurtosis) of the time series behavior of the first two components

	One month		Three months		Six months	
	1st PC	2nd PC	1st PC	2nd PC	1st PC	2nd PC
Minimum	−5.05	−6.24	−5.93	−4.40	−6.09	−3.61
Maximum	6.23	6.74	5.35	3.95	4.97	4.08
Skewness	0.03	0.14	−0.01	0.03	−0.06	0.32
Kurtosis	10.42	11.30	9.45	4.94	8.08	4.72

Skiadopoulos et al. (1999) had explored the dynamics of the CME S&P 500 implied volatilities for 1992–1995. They found that two components move implied volatilities, as well. So far, it is well understood that at any *given point in time*, implied distributions, implied volatilities, and option prices convey the same information. ''Heavy'' tailed implied distributions are mapped to implied volatility smiles; equivalently stated, the Black–Scholes option model underprices away from-the-money options, and overprices close to-the-money options. Our results show that the *evolution* of implied distributions and that of implied volatilities is affected by the same number of factors. However, the interpretation of the CDF obtained components is not intuitive. To obtain a simple interpretation we resorted to the ''Procrustes'' type rotation developed by Skiadopoulos et al. (1999).

In a ''Procrustes'' rotation the initially obtained correlation loadings are rotated so as to fit a targeted interpretation (see Jackson, 1991, for a description). Intuitively, we would expect that changes in implied distributions stem from changes in their moments (Skiadopoulos and Hodges, 2001). Positive changes in the mean would shift distributions to the left (right). Changes in the variance and kurtosis would shrink distributions and make them heavy-tailed. If the first PC had correlation loadings of equal size and of the same sign, then it would move the initial PDF to the left (or to the right, if the shock was negative). In such a case, the first PC could be interpreted as a shock to the mean. We could interpret the second PC as a shock to the variance, or to the kurtosis, if it's correlation loadings increase and then decline. Skiadopoulos et al. (1999) use the Procrustes rotation to make the first PC to be close to a parallel shift, as possible. [8] The technique is based on a regression that is performed so as to find the orthogonal rotation which minimizes the least squares distance between the loadings of the first PC and a vector of constants. However, the rotation was not successful; it simply interchanged the first and second PCs correlation loadings. Hence, we decide not to report the rotation results.

[8] The first PC cannot move CDFs in an exact parallel fashion, since this would make the perturbed PDF to integrate to more than one. Other rotation methods such as the varimax, the quartimax and the oblique, can not give us the desired intuitive interpretation (see Jackson, 1991). This is the reason we choose to apply a Procrustes rotation.

5. Simulating the implied probability density function: The algorithm

In this section, we present a new algorithm for Monte Carlo simulation of the implied PDF. The suggested simulation method is easy to implement because it does not require calculating the drift term of the process. It requires as inputs a starting value, and the number and form of shocks (volatility coefficients) of the process. The starting point is the extracted from the observed option prices implied distribution. The volatility coefficients of the process can be estimated by performing PCA on implied distributions. The algorithm for the Monte Carlo simulation of the implied CDF is discussed in Section 6.

5.1. The general idea

Breeden and Litzenberger (1978) first showed that the formed at current time t probability $\pi_t(X(\delta), T)$ can be extracted from the market call option prices observed across a continuum of strikes at time t, $\forall X(\delta)$. Knowing the next time step $t+1$ implied risk neutral probability $\pi_{t+1}(X(\delta), T)$ for $\forall X(\delta)$, would enable us to answer questions about the smile-consistent pricing and hedging of European style options, and forecasting future VaR levels.

Monte Carlo (MC) simulation appears as the natural tool for the implementation of the above idea. MC can be performed on the implied PDF, or equivalently on the implied CDF. However, the simulation has to be subject to certain constraints. In the case that one chooses to simulate the implied PDF, the MC simulation needs to be performed in a way so as to guarantee (a) an arbitrage-free evolution of the implied probabilities, (b) that the simulated implied density integrates to one at every time step of the simulation, and (c) the simulated $\pi_t(X(\delta), T)$ is non-negative.

5.2. The arbitrage-free evolution of the probabilities

Let the probabilities evolve obeying the diffusion process

$$\frac{\mathrm{d}\pi_t(X(\delta), T)}{\pi_t(X(\delta), T)} = a(X(\delta), T)\,\mathrm{d}t + \sum_{j=1}^{r} f_j(X(\delta), T)\,\mathrm{d}B_{j,t}, \tag{3}$$

where r is the number of factors, T is the PDF's expiry date, and B_j is the jth Brownian motion with $\mathrm{Cor}(\mathrm{d}B_i, \mathrm{d}B_j) = 0$, for $i \neq j$. The notation indicates that the jth factor depends on T. Hence, in our framework $f_j(X(\delta), T)$ is the PCA correlation loading estimated for a particular delta and expiry date, and B_j is the jth retained principal component $(j = 1, 2)$.

The simulation has to be carried out by requiring that the simulated probabilities are martingales under the risk-neutral measure. Hence, when their expectation is taken with respect to the equivalent martingale measure conditional on the information at time t, the following property holds:

$$E_t^*[\pi_s(X(\delta), T)] = \pi_t(X(\delta), T) \tag{4}$$

for $t < s$, i.e. today's 30-day PDF/CDF is an unbiased predictor of tomorrow's 29-day PDF/CDF under the risk-neutral measure.

The martingale condition follows from the law of iterated expectations (see Skiadopoulos and Hodges, 2001). [9] Intuitively, it is expected to hold since the risk-neutral probability can be viewed as the price of a forward contract written on an Arrow–Debreu security; the forward price of any asset is a martingale under the risk-neutral measure. The martingale property ensures that any arbitrage opportunities are excluded. The arbitrage-free property is particularly important in the case that the proposed algorithms are used for option pricing purposes; it ensures that the Merton's standard no-arbitrage results hold.

It follows that Eq. (3) has to be modified so as probabilities to evolve as martingales. The following proposition shows the appropriate transformation.

Proposition 1. *The process*

$$\frac{\mathrm{d}\pi_t(X(\delta),T)}{\pi_t(X(\delta),T)} = \sum_{j=1}^{r} f_j(X(\delta),T)\,\mathrm{d}B_{j,t} \tag{5}$$

ensures that the simulated PDF evolves as a martingale.

Proof. This is a standard result; any random variable is a martingale assuming that its relative changes follow a driftless Geometric Brownian Motion. □

Notice that Proposition 1 holds only for *fixed expiry date* distributions. This is because the maturity date T needs to be fixed for PDFs/CDFs to follow a martingale. In contrast, constant-maturity distributions do not need to follow a martingale. In this case, the driftless process in Eq. (5) cannot be used. However, the empirical evidence in Section 3, shows that constant-maturity distributions evolve as martingales and therefore Proposition 1 can also be applied to constant-maturity CDFs. In this case, T corresponds to a particular constant horizon, and $f_j(X(\delta),T)$ is the PCA correlation loading estimated for a particular delta and constant horizon.

Proposition 1 delivers the driftless process (5) that can be used (in principle) to simulate the implied PDF. In contrast to models that estimate the evolution of implied or local volatilities (e.g., Ledoit and Santa-Clara, 1998; Derman and Kani, 1998), the simulation can be performed easily because no drift has to be estimated. The drift has to vanish so as to ensure that no-arbitrage opportunities arise. However, Eq. (5) has to be modified further so as to exclude the occurrence of negative simulated probabilities.

5.3. Integration of probabilities to one

The simulation algorithm has to ensure that the simulated PDF integrates to one at every time step of the simulation. The initial density at time $t = 0$, integrates to

[9] More generally, the martingale condition is based on the general property of conditional probabilities with a complete partition.

one. However, this is not necessarily true for the simulated PDF for future times s $(0 < s < T)$. The random numbers used to perturb the initial density may produce a new density that integrates to more or less than one. We can accommodate the issue of the integration of the simulated PDF to one due to the linearity of Eq. (5). The following proposition shows how to do this.

Proposition 2. *Given that the probability distribution integrates to one at the current time t it will also integrate to one in every time step of the simulation s, $t < s < T$, if we use the process*

$$\pi_{t+1}(X(\delta), T) = \pi_t(X(\delta), T)\left\{1 + \sum_{j=1}^{r}[f_j(X(\delta), T) - \mu_j]\,\mathrm{d}B_{j,t}\right\}, \tag{6}$$

where $\mu_j = \sum_{k=1}^{\infty} \pi_t(X(\delta_k), T) f_j(X(\delta_k), T)$.

Proof. Available from the authors upon request. □

Corollary 1. *In order to ensure non-negative probabilities we must have*

$$\sum_{j=1}^{r}[f_j(X(\delta), T) - \mu_j]\,\mathrm{d}B_{j,t} \geqslant -1, \ \forall X(\delta). \tag{7}$$

Proof. It follows directly from Eq. (6). □

Using the *linear* stochastic differential equation (6) allows us to force the simulated density to integrate to one, and to accommodate for non-negative probabilities. This would not be the case if we had used the exponential solution of Eq. (5).

However, Corollary 1 poses numerical problems to the implementation of the simulation. For every $X(\delta)$, appropriate random numbers have to be generated so that Corollary 1 is satisfied. This would imply that different shocks occur *at the same time*, each one affecting different point of the PDF. However, in our analysis, we consider that at a certain point in time *one shock* occurs; its impact on every point of the PDF is different, and it is quantified by the corresponding correlation loading. We circumvent this obstacle by performing the simulation using the solution of Eq. (6), i.e.

$$\pi_{t+\Delta t} = \pi_t \times \exp\left\{-\frac{1}{2}\sum_{j=1}^{r}[f_j(X(\delta), T) - \mu_j]^2 \Delta t + \sum_{j=1}^{r}[f_j(X(\delta), T) - \mu_j]\Delta B_{j,t}\right\}. \tag{8}$$

The exponential term of Eq. (8) ensures that the simulated probabilities will be always positive.

6. Simulating the implied cumulative distribution function: The algorithm

In this section, we develop a new algorithm for Monte Carlo simulation of the implied CDF. The simulation algorithm has to ensure that the simulated state cumulative probabilities lie between zero and one. In addition, the simulated probabilities have to evolve as a martingale as it was the case with the simulated implied PDF. On the other hand, the simulated CDF does not have to integrate to one.

The initial probabilities at time $t = 0$ fall between zero and one, by construction. However, this is not necessarily true for the simulated probabilities for future times s $(0 < s < T)$. To ensure that the simulated probabilities will lie in the interval [0,1] we simulate first a non-linear transformation of the probabilities, and then we switch to the corresponding simulated probability.

In particular, we define a new variable $y_t \equiv \Phi^{-1}(\pi_t)$, where $\Phi(\cdot)$ is the cumulative standard normal distribution function (the arguments $X(\delta)$ and T are suppressed for simplicity). The variable y_t can be thought of as the strike price of a hypothetical normal distribution, corresponding to a given delta and maturity. Irrespective of the value that y_t gets, π_t will be between zero and one. Hence, we simulate the defined variable y_t and then we convert it to the corresponding value of π_t. This ensures that the simulated cumulative probabilities will lie between 0 and 1. The following proposition derives the no-arbitrage process for y_t.

Proposition 3. *The variable y_t follows the process*

$$\mathrm{d}y_t = \frac{1}{2} y_t \frac{\Phi(y_t)^2}{\phi(y_t)^2} \left(\sum_{j=1}^{r} f_j^2 \right) \mathrm{d}t + \frac{\Phi(y_t)}{\phi(y_t)} \sum_{j=1}^{r} f_j \, \mathrm{d}B_{j,t}, \tag{9}$$

where $\phi(y_t)$ is the standard normal probability density function of y_t, and $\Phi(y_t)$ is the cumulative standard normal distribution.

Proof. Available from the authors upon request. □

7. A test of the out-of-sample performance

In this section, we test the out-of-sample performance of the CDF simulation algorithm within a VaR framework. We calculate VaR using the E-VaR measure proposed by Ait-Sahalia and Lo (2000). E-VaR is defined similarly to the conventional VaR (Ait-Sahalia and Lo call the latter Statistical VaR, S-VaR); it is the percentile (loss) that corresponds to a given probability and time horizon. However, E-VaR is calculated from the risk-neutral distribution, while S-VaR is estimated from the actual distribution. E-VaR is a more general measure risk since it incorporates the investor's risk preferences, the demand–supply effects, and the probabilities that correspond to extreme losses. Hence, it is determined by the three P's (preferences, prices, and probabilities) that any complete risk management system should take into account (see Lo, 1999). On the other hand, S-VaR is just a statistical evaluation

of uncertainty. The ratio of S-VaR and E-VaR measures the market participants' risk aversion. S-VaR and E-VaR are identical in the special case that investors are risk-neutral and rational.

Given an initial constant-maturity E-VaR, we use the CDF algorithm and the PCA results to forecast the VaR's variability over time by constructing confidence intervals. Bliss and Panigirtzoglou (in press) have found that the risk-neutral PDF variability (e.g. E-VaR variability) is similar to that of the subjective PDF (e.g. S-VaR variability); their results are robust to different maturities and to different specifications of the utility function. Since the test focuses on VaR variability, we expect that the distinction between E-VaR and S-VaR is not important.

7.1. The test

Conventionally, any measure of VaR is defined in terms of the loss associated with a particular probability level (*dollar VaR*). However, since our data set contains probabilities, we specify E-VaR in the *equivalent reverse* way, i.e. in terms of the probability that corresponds to a particular loss (e.g. the loss level that corresponds to a call delta of 0.941 – *probability VaR*).

The application is structured as follows: let a sample of K extreme probabilities $\pi_t(X(\delta), T)$, $t = 0, 1, \ldots, K$. We start from an initially observed extreme probability and we simulate it for the next n days (n-simulation horizon) using Eq. (9) and the corresponding PCA constant-maturity correlation loadings as volatility coefficients. We store the nth simulated extreme probability. Then, we take as an initial point, the extreme $(n+1)$ probability of our sample and we repeat the simulation for the next n days; we store the $(2n+1)$ simulated probability. The simulation terminates at the $(K-n)$ observation. At the end, we have stored $(K-n)/n$ simulated extreme probabilities. We repeat the simulation exercise 1000 times (runs). Finally, for each one of the stored simulated extreme probabilities, we calculate the standard deviation across the 1000 runs.

The mean of each one of the stored probabilities across the 1000 runs is the corresponding initial (today's) probability VaR, by construction of the algorithm (simulated probabilities evolve as martingales). In addition, the simulated probability E-VaR is distributed normally since we use Brownian shocks. Then, for a level of significance $a\%$, we can construct $(1-a)\%$ confidence intervals for the future probability VaR by adding/subtracting from the mean the appropriate number m of standard deviations, as follows:

$$\pi_i(X(\delta), T) - m\sigma_{i+n} < \pi_{i+n}(X(\delta), T) < \pi_i(X(\delta), T) + m\sigma_{i+n}, \tag{10}$$

where $i = 0, n, \ldots, K-n$, σ_{i+n} is the standard deviation of the $i+n$ date probability E-VaR, and $\pi_{i+n}(X(\delta), T)$ is the $(i+n)$ date realized probability E-VaR, as a function of delta. For example, the algorithm predicts that the probability E-VaR to be realized after 14 days will fall within the two 95% confidence limits. In this respect, the calculated (simulated) standard deviation measures the probability E-VaR's variability.

In the case that the $(1-a)\%$ of the $(K-n)/n$ realized probabilities falls between the upper and lower confidence limits, the algorithm will forecast accurately the variation of tomorrow's E-VaR. These conclusions are based both on the historically estimated correlations loadings and on the way the algorithm is constructed.

7.2. Implementation issues

We test the out-of-sample performance of the algorithm using the S&P 500 implied CDF data for the year 2001. For each one of the three constant-horizon CDFs, we simulate the extreme probability of delta equal to 0.941 for a 14-days simulation horizon. Hence, the goal is to forecast the variability of the probability E-VaR over the next 14 days, every 14 days in year 2001. The number of observations in our sample is 238. Therefore, for each simulation run we store 16 values.

A potential limitation to implementing the test is the lack of traded away from-the-money strikes; this may hamper the accurate estimation of the left tail of the implied distribution to which the 0.941 call delta corresponds. However, in our analysis we have estimated the left tail of implied distributions using out-of-the-money puts. These options are traded even for deep out-of-the-money strikes that correspond to the region between 0.97 and 0.99 delta.

In principle, the simulation is carried out via Eq. (9). However, implementation-wise, there are two issues we should take into account. First, the factors $f_j^{\mathrm{PCA}}(X(\delta),T)$ are extracted from applying PCA to the *changes* of cumulative probabilities. Therefore, they are related to the factors $f_j(X(\delta),T)$ in Eq. (5) via

$$f_j^{\mathrm{PCA}}(X(\delta),T) = f_j(X(\delta),T)\pi_t(X(\delta),T) \rightarrow f_j^{\mathrm{PCA}}(X(\delta),T) = f_j(X(\delta),T)\Phi(y_t).$$

Hence, Eq. (9) should be used as

$$\mathrm{d}y_t = \frac{1}{2}y_t\frac{1}{\phi(y_t)^2}\left(\sum_{j=1}^{r}(f_j^{\mathrm{PCA}})^2\right)\mathrm{d}t + \frac{1}{\phi(y_t)}\sum_{j=1}^{r}f_j^{\mathrm{PCA}}\,\mathrm{d}B_{j,t}. \tag{11}$$

The simulation of the implied CDF can be performed by discretizing Eq. (11) using a standard Euler discretization scheme.

The second issue is that the correlation loadings have been estimated by performing PCA on the standardized variables $\Delta\pi_t(X(\delta),T)$. However, the simulation refers to unstandardized variables. Therefore, in Eq. (11) the factors $f_j^{\mathrm{PCA}}(X(\delta),T)$ should be scaled by multiplying them with the standard deviations $\sigma(X(\delta),T)$ of the corresponding variable $X(\delta)$.

7.3. Discussion of the results

The probability E-VaR confidence interval is translated to a dollar E-VaR confidence interval. For any given delta, we map the lower and upper confidence limit of the confidence interval (Eq. (10)) to the corresponding (strike) E-VaR level. The transformation is done via Black's delta. Figs. 2–4 provide a visual test of the predictive power of the constructed probability E-VaR confidence intervals for each one of

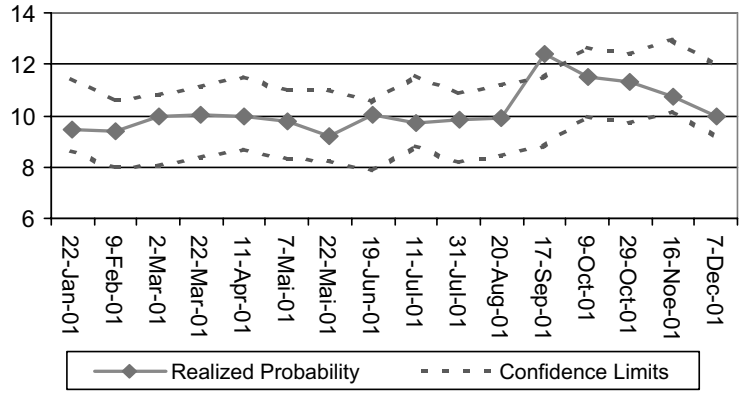

Fig. 2. One-month realized 0.941 delta probability and simulated 95% confidence intervals.

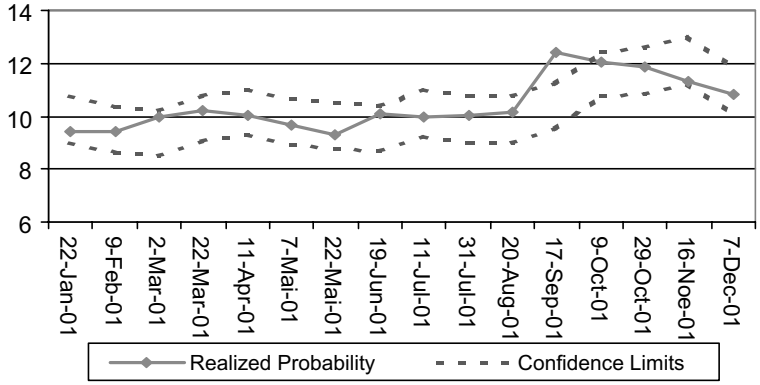

Fig. 3. Three-months realized 0.941 delta probability and simulated 95% confidence intervals.

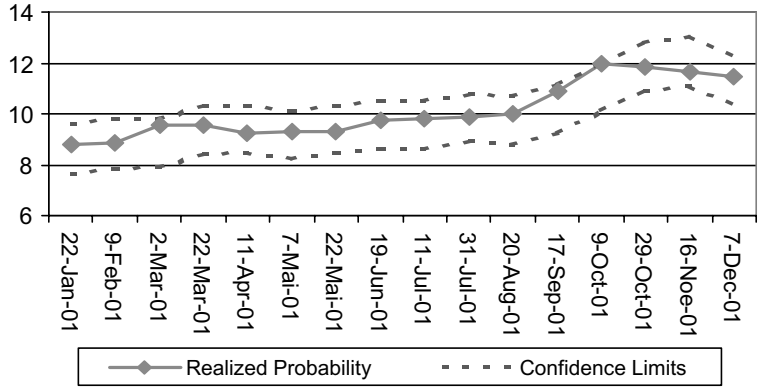

Fig. 4. Six-months realized 0.941 delta probability and simulated 95% confidence intervals.

the three maturities. The figures show the realized 0.941 delta probability E-VaR, and the simulation-based upper and lower confidence limits of the 95% confidence interval across the monitoring dates (probabilities have been multiplied by 100).

We can see that the realized probability VaR falls within the constructed confidence interval for all but one the monitoring dates. The exception is the realized probability on the 17th September, 2001, for the one and three-month's maturity. Inspection of the data reveals that this is due to the 11th September crash that made the subsequent short horizon implied distributions more negatively skewed (the 17th September simulated confidence interval has as a starting point the 21st August implied distribution). However, the implied distribution for the six-months horizon was not affected by the crash, as much as the shorter horizon distributions. This reflects the (risk-neutral) investors' perception that the probability of a further decline after the crash was higher only for shorter horizons.

The fact that the simulated intervals "miss" one observation is expected. This is because these are 95% confidence intervals; we expect that almost one out of sixteen observations will lie out of these intervals. Therefore, the simulated confidence interval forecast accurately the range within the S&P500 probability E-VaR will lie in year 2001. This holds regardless of the starting point. Approximating the volatility structure of the normal Brownian shocks appearing in Eq. (9) with the correlation loadings of the non-normal components does not affect the performance of the method, either. The fact that the normal shocks used in the algorithms do not account for the excess kurtosis of the two retained components, does not affect the accuracy of the derived confidence limits.

8. Conclusions and implications of the research

We proposed and implemented a new approach to model the evolution of implied distributions over time. First, we investigated the dynamics of the S&P 500 implied cumulative distribution functions, by applying PCA. The Bliss and Panigirtzoglou (2002) method has been used in order to extract the implied distributions. Our study has been performed for one, three, and six-month constant horizons implied distributions. The results provide important insights into the evolution of implied distributions and allow its parsimonious modeling as a diffusion process. The second contribution of the paper is the development of methods to model the implied distribution as a diffusion process. Two new Monte Carlo simulation methods have been presented. These simulate the evolution of the implied PDF and that of the implied CDF over time, respectively. The out-of-sample performance within a VaR framework is examined.

We considered three alternative criteria (Velicer's criterion, communalities, interpretation) to decide on the number of components driving implied distributions. We found that two components account for the CDF evolution over time in each one of the three maturities. These explain on average about 90% of the CDF's variance across the three maturities. The proposed simulation methods are arbitrage-free, and they can be implemented easily. They are based on a diffusion process that

describes the evolution of the implied distribution. They require as inputs only the initial implied distribution, and the volatility structure that is estimated by PCA. Finally, we have provided a joint test of the out-of-sample performance of the PCA results and of the CDF algorithm by using the E-VaR measure proposed by Ait-Sahalia and Lo (2000). The results show that the algorithm forecasts accurately the interval within which the S&P 500 probability E-VaR will lie over the next 14 days in year 2001. These findings are robust to the choice of the VaR horizon, and to the choice of the initial probability VaR, as a starting point for the simulation.

The results from the out-of-sample test have implications for the economics of option pricing. Dumas et al. (1998) have examined the out-of-sample performance of "smile-consistent" deterministic volatility models. They performed their study by considering the stability of implied deterministic volatility functions for the S&P 500 index. They found that *deterministic* volatility models cannot predict the evolution of option prices. Our results indicate that a more general "smile-consistent" model where all the moments change *stochastically* may be the appropriate approach to capture the dynamics of option prices.

This paper creates two strands for future research. First, the empirical issue of the dynamics of implied distributions should be explored further by using different data sets/different time periods and by employing different methods. It may be the case that the number and shape of shocks that affect implied distributions, depend on the underlying asset, just as it is the case with the dynamics of implied volatilities. Second, researchers should assess the contribution of the suggested algorithms in a number of applications. The algorithms allow the construction of (arbitrage) bounds to option prices. This can be particularly useful for the construction of bounds to the prices of exotic options, complementing recent work by Hodges and Neuberger (2001). Also, trading strategies that aim to profit from changes in higher-order moments (e.g. skewness and kurtosis trades) can be designed (see Ait-Sahalia et al., 2001, for such strategies). Alternative processes such as a jump-diffusion process for the evolution of implied distributions should also be considered. This will be necessary so as to capture any discontinuities in the underlying asset price.

Acknowledgements

We are indebted to Stewart Hodges for the inspiration he provided. We would also like to thank Karim Abadir, Carol Alexander, Robert Bliss, Peter Carr, George Constandinides, Jens Jackwerth, George Kapetanios, Anastassios Malliaris, Anthony Neuberger, Joao Pedro Nunes, Riccardo Rebonato, Olivier Renault, Michael Rockinger, Pedro Santa-Clara, Phillip Schönbucher, Robert Tompkins, Dimitris Vayanos, Stavros Zenios, William Ziemba, and the participants at the 2002 FEES Conference (Athens), the 2002 Bachelier World Congress (Crete), the 2002 FORC Conference (Warwick), the 2002 EIR Conference (LSE), the 2002 Quantitative Finance Conference (London), the Athens University of Economics and Business, the University of Piraeus, and the ISMA Research Centre seminars for many helpful

discussions and comments. We are grateful to two anonymous referees for their thorough and constructive comments. The views expressed herein are those of the authors and do not necessarily reflect those of the Bank of England. Any remaining errors are our responsibility alone.

References

Ait-Sahalia, Y., Lo, A.W., 2000. Nonparametric risk management and implied risk aversion. Journal of Econometrics 94, 9–51.

Ait-Sahalia, Y., Wang, Y., Yared, F., 2001. Do option markets correctly price the probabilities of movement of the underlying asset? Journal of Econometrics 102, 67–110.

Alexander, C.O., 2001a. Principles of the skew. Risk 14, 29–32.

Alexander, C.O., 2001b. Market models: A guide to financial data analysis. John Wiley & Sons Ltd.

Ané, T., Labidi, C., 2001. Implied volatility surfaces and market activity over time. Journal of Economics and Finance 25, 259–275.

Barone-Adesi, G., Whaley, R.E., 1987. Efficient analytical approximation of American option values. Journal of Finance 42, 301–320.

Basilevsky, A., 1994. Statistical Factor Analysis and Related Methods: Theory and Applications. In: Wiley Series in Probability and Mathematical Statistics. John Wiley & Sons Ltd.

Bates, D.S., 1991. The Crash of '87: Was it expected? The evidence from options market. Journal of Finance 46, 1009–1044.

Bates, D.S., 1996. Jumps and stochastic volatility: Exchange rate processes implicit in Deutsche Mark options. Review of Financial Studies 9, 69–107.

Bates, D.S., 2003. Empirical option pricing: A retrospection. Journal of Econometrics 116 (1/2), 387–404.

Bliss, R., Panigirtzoglou, N., 2002. Testing the stability of implied probability density functions. Journal of Banking and Finance 26, 381–422.

Bliss, R., Panigirtzoglou, N., in press. Option-implied risk aversion estimates. Journal of Finance.

Breeden, D., Litzenberger, R., 1978. Prices of state-contingent claims implicit in option prices. Journal of Business 51, 621–651.

Britten-Jones, M., Neuberger, A., 2000. Option prices, implied price processes, and stochastic volatility. Journal of Finance 55, 839–866.

Buraschi, A., Jackwerth, J.C., 2001. The price of a smile: Hedging and spanning in option markets. Review of Financial Studies 14, 495–527.

Clews, R., Panigirtzoglou, N., Proudman, J., 2000. Recent developments in extracting information from option markets. Bank of England Quarterly Bulletin 40, 50–60.

Cont, R., Da Fonseca, J., 2002. Dynamics of implied volatility surfaces. Quantitative Finance 2, 45–60.

Coutant, S., Jondeau, E., Rockinger, M., 2001. Reading PIBOR futures options smiles: The 1997 snap election. Journal of Banking and Finance 25, 1957–1987.

Dumas, B., Fleming, J., Whaley, R.E., 1998. Implied volatility functions: Empirical tests. Journal of Finance 53, 2059–2106.

Derman, E., Kani, I., 1998. Stochastic implied trees: Arbitrage pricing with stochastic term and strike structure of volatility. International Journal of Theoretical and Applied Finance 1, 61–110.

Fama, E., French, K., 1992. The cross-section of expected stock returns. Journal of Finance 47, 427–465.

Fengler, M.R., Härdle, W.K., Villa, C., 2001. The dynamics of implied volatilities: A common principal components approach. Working Paper 38, Humboldt University, Berlin, June.

Frachot, A., Jansi, D., Lacoste, V., 1992. Factor analysis of the term structure: A probabilistic approach. Working paper, Bank of France.

Gemmill, G., Saflekos, A., 2000. How useful are implied distributions? Evidence from stock-index options. Journal of Derivatives 7, 83–98.

Harvey, C.R., Whaley, R.E., 1991. S&P 100 index option volatility. Journal of Finance 46, 1551–1561.

Harvey, C.R., Siddique, A., 2000. Conditional skewness in asset pricing tests. Journal of Finance 55, 1263–1295.

Heath, D., Jarrow, R., Morton, A., 1992. Bond pricing and the term structure of interest rates: A new methodology for contingent claims valuation. Econometrica 60, 77–105.

Hodges, S.D., Neuberger, A., 2001. Rational bounds on exotic options. Working paper, Financial Options Research Centre, University of Warwick.

Jackson, E., 1991. A User's Guide to Principal Components. Wiley Series in Probability and Mathematical Statistics. John Wiley and Sons Ltd.

Jackwerth, J.C., 1999. Implied binomial trees: A literature review. Journal of Derivatives 7, 66–82.

Kamal, M., Derman, E., 1997. The Patterns of Change in Implied Index Volatilities. Quantitative Strategies Research Notes. Goldman Sachs, New York.

Knez, P.J., Litterman, R., Scheinkman, J., 1994. Explorations into factors explaining money market returns. Journal of Finance 49, 1861–1882.

Kyle, A.S., 1985. Continuous auctions and insider trading. Econometrica 51, 1315–1335.

Ledoit, O., Santa-Clara, P., 1998. Relative pricing of options with stochastic volatility. Working paper, University of California, Los Angeles.

Lynch, D., Panigirtzoglou, N., 2003. Summary Statistics of Option-Implied Probability Density Functions and their Properties. Mimeo., Bank of England.

Lo, A.W., 1999. The three P's of total risk management. Financial Analysts Journal 55, 13–26.

Malz, A., 1997. Estimating the probability distribution of future exchange rates from option prices. Journal of Derivatives 5, 18–36.

Mayhew, S., 1995. On estimating the risk-neutral probability distribution implied by option prices. Working paper, University of California, Berkeley.

McIntyre, M., 2001. Performance of Dupire's implied diffusion approach under sparse and incomplete data. Journal of Computational Finance 4, 33–84.

Neuhaus, H.,1995. The information content of derivatives for monetary policy: Implied volatilities and probabilities. Economic Research Group Discussion paper, No. 3/95, Deutsche Bundesbank.

Schönbucher, P.J., 1999. A market model of stochastic implied volatility. Philosophical Transactions of the Royal Society, Series A 357, 2071–2092.

Skiadopoulos, G., Hodges, S.D., Clewlow, L., 1999. The dynamics of the S&P 500 implied volatility surface. Review of Derivatives Research 3, 263–282.

Skiadopoulos, G., 2001. Volatility smile consistent option models: A survey. International Journal of Theoretical and Applied Finance 4, 403–437.

Skiadopoulos, G., Hodges, S.D., 2001. Simulating the evolution of the implied distribution. European Financial Management Journal 7, 497–521.

Söderlind, P., Svensson, L., 1997. New techniques to extract market expectations from financial instruments. Journal of Monetary Economics 40, 383–429.

Velicer, W., 1976. Determining the number of components from the matrix of partial correlations. Psychometrica 41, 321–327.